Preprints of the 18th IFAC World Congress
Milano (Italy) August 28 - September 2, 2011

Stability Analysis of Multi-Fingered Grasp under Destabilizing Gravity Effect

Akira Nakashima * **Yoshikazu Hayakawa** *,**

* *Mechanical Science and Engineering, Graduate School of Engineering, Nagoya University, Furo-cho, Chikusa-ku, Nagoya, Japan (e-mail: a_nakashima@nuem.nagoya-u.ac.jp)*
** *RIKEN-TRI Collaboration Center, RIKEN, 2271-103, Anagahora, Shimoshidami, Moriyama-ku, Nagoya, Japan.*

Abstract: In this paper, we deal with the stability analysis of an object grasped by fingers with linear stiffness in the case where the gravity effect is considered. The stability of the grasp is defined based on the potential energy of the grasp. The analysis problem is formulated as finding a condition of the stiffness parameters and contact points for the position of the center of gravity (COG) to exist such that the grasp is stable. A necessary and sufficient condition is derived under assumptions with respect to the stiffness and contact points. Furthermore, on the derived condition, the position of the COG is characterized with respect to the stiffness and contact points. It is especially indicated that the grasp can be stable with any position of the COG. Numerical examples are shown to prove the effectiveness of the analysis.

Keywords: robotics, handling, robot control, springs, stability analysis

1. INTRODUCTION

Many researchers have tried to introduce robots into human's daily life environments. Since the robots are aimed to do various tasks instead of humans, multi-fingered robot hands are effective as end-effectors because they have capability to grasp and manipulate variously-shaped objects with multi contacts and multi joints. Especially, the stable grasp is more important than the manipulation because it has to be established primarily and eternally. The stable grasp has been dealt with from the viewpoints of the statics, dynamics and quasi-statics.

The stable grasp with the statics means the analysis and optimization of the factors, i.e., the grasping forces, the contact points and the configurations of the object and fingers. The optimized factors with criteria in some major studies are allowable grasping forces within the set due to the friction and torque limitations by Kerr and Roth (1986); the grasping forces with a safety factor to prevent the break of the object by Nakamura et al. (1989); the grasping forces with a force decomposition based on a clear physical meaning by Yoshikawa and Nagai (1991); the contact points with allowable disturbance forces based on the Force-Closure, e.g., by Nguyen (1988), Li and Sastry (1988), Markenscoff and Papadimitriou (1989) and Magialardi et al. (1996). Recently, all the factors are considered by Watanabe and Yoshikawa (2003) with sets of required external forces and acceleration. However, it is not considered how the grasping forces effect on the stability of the object motion to be perturbed since the grasp situation is static. Furthermore, appropriate control methods are necessary in order to establish the stable grasp because the optimization of the factors is only the enhancement of the stability margin.

The stable grasp with the dynamics is considered from the viewpoints of the computed torque law and the Lyapunov theory. The first one is a major control method in robotics and was initially used for the grasp and manipulation, e.g., Cole et al. (1989), Sarkar et al. (1997) and Zheng et al. (2000). The good summary is written in the book by Murray et al. (1994). The second one is a major stability theory in the control theory and has been studied, e.g., Nagai and Yoshikawa (1993), Cheah et al. (1998), Arimoto et al. (2002) and Nakashima et al. (2009). Recently, Arimoto (2008) proposed control methods with estimators of unknown object parameters. They call the grasp by their methods blind grasping because the methods does not need the measurements of the forces and contact points and the knowledge of the object. The stability of the closed whole system is proved based on the concept of stability on a manifold. However, as in the proof of the stability, the target values of the grasping forces and the estimator gains have to be appropriate values, conditions of which are explicitly not given. Therefore, those parameters should be determined by iterative trial and error.

The stable grasp with the quasi-statics is discussed based on the *stiffness-effect* (Cutkosky and Kao (1989)), which is the resultant force and moment due to the unbalanced grasping forces when the grasped object is perturbed from its equilibrium point. Hanafusa and Asada (1977) considered the grasp by fingers, each of which is assumed to be one degree of freedom (DOF) linear spring. They derived that a equilibrium of the grasp is stable when it is a strict local minimum of the elastic potential energy due to the fingers. This means that the stiffness effect by the grasping forces is the *restoring force* against the perturbation. This case was extended to the grasp with the two DOF springs by Kaneko et al. (1990). The case in 3D

space was discussed by Yamada et al. (2001). The effects of the rolling contact and the curvatures of the fingers and object were studied by Howard and Kumar (1996), Montana (1992) and Yamada et al. (2001). It is possible to obtain the stiffness and contact points analytically or numerically when the object parameters are given since the conditions of those parameters are explicitly derived in the studies. Therefore, the results of the analysis with the quasi-statics are feasible for the stable grasp since the stiffness can be relatively easily realized by any appropriate compliance or impedance controls, e.g., Nakashima et al. (2010). However, the *gravity effect* is ignored because of the complexity of the analysis with it though it can destabilize the grasp. It is intuitively obvious that the gravity effect is destabilizing factor for the grasp in the case where the center of gravity (COG) is above a center of rotation when the object is disturbed.

The COG of a grasped object is very important factor in the grasp stability with the object perturbation. As the stability of frictionless grasps to be neither the Force-Closure nor Form-Closure, there are the fixture of assembling objects by Mattikalli et al. (1995); Baraff et al. (1997) and nonprehensile manipulation by Abell and Erdmann (1995); Zumel and Erdmann (1996), where the grasping forces are constant and the quasi-static rotation of the objects are considered. The object region is investigated in which the gravity froce does not effect on the directions not to be generated by any fingers. As more realistic situation of frictional contacts, Svinin et al. (1999) analyzed the effect of the gravity for the stiffness of the grasped object with frictional constant grasping forces. However, it is a little improper to assume that the grasping forces and the contact locations on the object are constant.

In this paper, we deal with the stability analysis of an object grasped by fingers with linear stiffness in the case where the gravity effect is considered. The stability of the grasp is defined based on the potential energy of the grasp. The analysis problem is formulated as finding a condition of the stiffness parameters and contact points for the position of the COG to exist such that the grasp is stable. A necessary and sufficient condition is derived under assumptions with respect to the stiffness and contact points. Furthermore, on the derived condition, the position of the COG is characterized with respect to the stiffness and contact points. It is especially indicated that the grasp can be stable with any position of the COG. Numerical examples are shown to prove the effectiveness of the analysis.

2. PRELIMINARIES

2.1 Problem Setting

Consider an object grasped by ith virtual linear spring at ith contact points C_i $(i = 1, \cdots, n)$ as shown in Fig. 1. Σ_B is the base frame and Σ_O is the object frame fixed to the object. Σ_O is represented by the position vector $\boldsymbol{p}_O \in \mathbb{R}^3$ and the rotation matrix $\boldsymbol{R}_O \in \mathbb{R}^{3\times3}$ of Σ_O expressed in Σ_B. Σ_B and Σ_O are assumed to coincide to each other at the initial state without loss of generality. The contact C_i and the COG of the object are represented by ${}^O\boldsymbol{p}_{C_i} \in \mathbb{R}^3$ and ${}^O\boldsymbol{p}_g \in \mathbb{R}^3$ expressed in Σ_O. In the latter, vectors without left superscripts are expressed in Σ_B. The ith spring frame Σ_{S_i} is fixed to the space with the origin which coincides to C_i at the initial state in order to represent the spring displacements. $\boldsymbol{p}_{S_i} \in \mathbb{R}^3$ and $\boldsymbol{R}_{S_i} \in \mathbb{R}^{3\times3}$ are the position and orientation of Σ_{S_i}. The spring displacements $\boldsymbol{\delta}_i := [\delta_{x_i}\ \delta_{y_i}\ \delta_{z_i}]^{\mathrm{T}} \in \mathbb{R}^3$ are defined as the coordinates in Σ_{S_i}. $\delta_{*_i} > 0$ and $\delta_{*_i} < 0$ express the compression and extension from the natural thinning. Note that $*$ denotes x, y or z. The stiffness coefficients are denoted by $\boldsymbol{K}_i := \text{block diag}(k_{x_i}, k_{y_i}, k_{z_i}) \in \mathbb{R}^{3\times3}$.

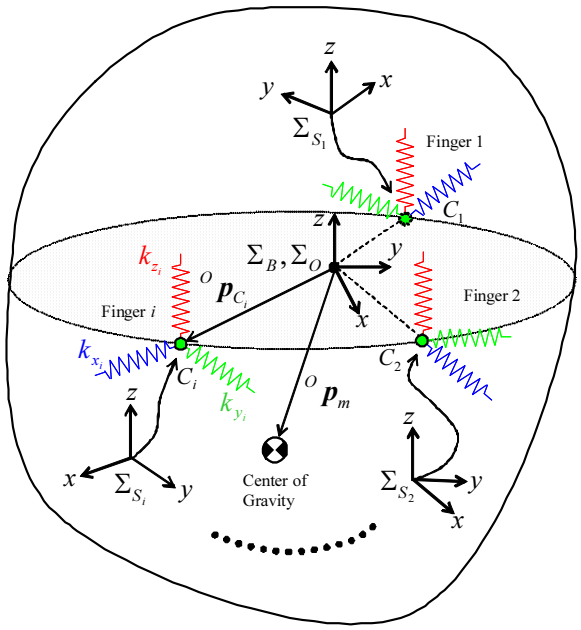

Fig. 1. An object grasped by virtual spring fingers.

We make the following assumptions:

Assumption 1. The x- and y-axes of the spring frame Σ_{S_i} are in the same plane and the elongations of all the x-axes cross at one point.

Assumption 2. The contact types are the fixed contact. Therefore, the contact C_i is not changed with respect to Σ_O.

Assumption 3. Σ_O is set to the cross point shown in Assumption 1. The x- and y-axes of Σ_O and Σ_{S_i} are in the same plane. The x-axis is set such that the COG is included in the (x, z)-plane.

Assumption 4. The grasping forces produced by the springs and the gravity force are balanced at the initial state.

Note that Σ_O can be fixed at any points of the object because the position and orientation of a frame fixed to the object are *equivalent* to *any* other frames fixed to the object. Therefore, Assumptions 3 and 4 are satisfied without loss of generality. From Assumptions 1–4, the following equations hold:

$$\sum_{i=1}^{n} \boldsymbol{f}_i^0 + m\boldsymbol{g} = \boldsymbol{0} \tag{1}$$

$$\sum_{i=1}^{n} \boldsymbol{p}_{C_i}^0 \times \boldsymbol{f}_i^0 + \boldsymbol{p}_g^0 \times m\boldsymbol{g} = \boldsymbol{0}, \tag{2}$$

where

$$\boldsymbol{f}_i^0 := -\boldsymbol{R}_{S_i}\boldsymbol{K}_i\boldsymbol{\delta}_{0_i}. \tag{3}$$

(1) and (2) denote the equilibrium of force and moment. $\boldsymbol{f}_i^0 \in \mathbb{R}^3$ is the initial force, m is the mass of the object, $\boldsymbol{g} := [0\ 0\ \ -g]^{\mathrm{T}} \in \mathbb{R}^3$, $g = 9.8$ [m/s^2] is the gravity vector. $\boldsymbol{\delta}_{0_i} := [\delta_{0x_i}\ \delta_{0y_i}\ \delta_{0z_i}]^{\mathrm{T}}$ are the initial of the spring displacements. $\boldsymbol{p}_{C_i}^0$ and $\boldsymbol{p}_g^0 \in \mathbb{R}^3$ are the initial contact point and the position of the COG given by

$$\begin{aligned} &\boldsymbol{p}_{C_i}^0 = \boldsymbol{p}_{S_i},\ \boldsymbol{p}_g^0 = {}^O\boldsymbol{p}_g \\ &\boldsymbol{p}_{S_i} := {}^O\boldsymbol{p}_{C_i},\ \boldsymbol{R}_{S_i} := \begin{bmatrix} C_{\alpha_i} & -S_{\alpha_i} & 0 \\ S_{\alpha_i} & C_{\alpha_i} & 0 \\ 0 & 0 & 1 \end{bmatrix} \\ &{}^O\boldsymbol{p}_{C_i} := [r_i C_{\alpha_i}\ r_i S_{\alpha_i}\ 0]^{\mathrm{T}} \\ &{}^O\boldsymbol{p}_g := [r_g S_{\beta_g}\ 0\ r_g C_{\beta_g}]^{\mathrm{T}}. \end{aligned} \tag{4}$$

From Assumption 2, note that $\boldsymbol{p}_{S_i}$ is a constant. r_*, α_* and β_* are the polar coordinates, where α_* and β_* are the angles from the x- and z-axes and $*$ denotes i or g. The ranges are $-\pi \le \alpha_* \le \pi$ and $0 \le \beta_* \le \pi$. From Assumption 1 and 3, note that $\beta_i = 0$ and $\alpha_g = 0$. For simplicity, the abbreviations $C_{\alpha_i} := \cos\alpha_i$, $S_{\alpha_i} := \sin\alpha_i$, $C_{\beta_g} := \cos\beta_g$ and $S_{\beta_g} := \sin\beta_g$ are used in the latter.

2.2 Stability Definition

For the grasp, we define the stability when the object is perturbed from the equilibrium with any small displacement $\boldsymbol{r} \in \mathbb{R}^6$. The perturbation $\boldsymbol{r}$ is expressed by the position $\boldsymbol{p}_O$ and the roll-pitch-yaw orientation $\boldsymbol{\phi}_O \in \mathbb{R}^3$ of $\boldsymbol{R}_O$ as $\boldsymbol{r} := [\ \boldsymbol{p}_O^{\mathrm{T}}\ \ \boldsymbol{\phi}_O^{\mathrm{T}}\ ]^{\mathrm{T}} \in \mathbb{R}^6$. The potential energy of the grasp is given by

$$U(\boldsymbol{r}) = \frac{1}{2}\sum_{i=1}^n \boldsymbol{\delta}_i(\boldsymbol{r})^{\mathrm{T}} \boldsymbol{K}_i \boldsymbol{\delta}_i(\boldsymbol{r}) - \boldsymbol{p}_g(\boldsymbol{r})^{\mathrm{T}} m\boldsymbol{g}, \tag{5}$$

where

$$\begin{aligned} \boldsymbol{\delta}_i(\boldsymbol{r}) &= \boldsymbol{R}_{S_i}^{-1}\{(\boldsymbol{R}_O(\boldsymbol{\phi}_O) - \boldsymbol{I}_3)^O\boldsymbol{p}_{C_i} + \boldsymbol{p}_O\} + \boldsymbol{\delta}_{0_i} \\ \boldsymbol{p}_g(\boldsymbol{r}) &= (\boldsymbol{R}_O(\boldsymbol{\phi}_O) - \boldsymbol{I}_3)^O\boldsymbol{p}_g + \boldsymbol{p}_O. \end{aligned} \tag{6}$$

The grasp stability is defined via $U(\boldsymbol{r})$ as:

Definition 1. The grasp is stable if $\boldsymbol{r} = \boldsymbol{0}$ is a strict local minimum of the potential energy $U(\boldsymbol{r})$.

Suppose $U(\boldsymbol{r}) \in C^2$. Then, Definition 1 yields the stability condition:

$$\nabla U(\boldsymbol{0}) = \boldsymbol{0},\ \nabla^2 U(\boldsymbol{0}) \succ 0. \tag{7}$$

The first condition of (7) is satisfied by (1) and (2). Therefore, the second condition is investigated in the latter.

2.3 The Stability Analysis Problem

$\nabla^2 U(\boldsymbol{0}) \in \mathbb{R}^{6\times 6}$ is related to the stiffness effect produced by the springs as Hanafusa and Asada (1977):

$$\boldsymbol{F}_r = -\boldsymbol{K}_r \boldsymbol{r}, \tag{8}$$

$$\boldsymbol{K}_r := \begin{bmatrix} \boldsymbol{K}_r^{pp} & \boldsymbol{K}_r^{p\phi} \\ \boldsymbol{K}_r^{p\phi} & \boldsymbol{K}_r^{\phi\phi} \end{bmatrix} = \nabla^2 U(\boldsymbol{0}), \tag{9}$$

where $\boldsymbol{F}_r \in \mathbb{R}^6$ is the stiffness effect and $\boldsymbol{K}_r \in \mathbb{R}^{6\times 6}$ is the *stiffness matrix*. Note that (7) and (8) imply $\boldsymbol{r}^{\mathrm{T}}\boldsymbol{F}_r = -\boldsymbol{r}^{\mathrm{T}}\boldsymbol{K}_r\boldsymbol{r} < 0$. Therefore, $\boldsymbol{F}_r$ is called as the *restoring force* when the grasp is stable. $\boldsymbol{K}_r^{pp}$ represents the stiffness effect from the position to the translational force and is always positive definite Kaneko et al. (1990). $\boldsymbol{K}_r^{p\phi}$ represents the coupling between the position and orientation, which can be calculated as $\boldsymbol{K}_r^{p\phi} = \boldsymbol{0}_{3\times 3}$ by Assumptions 1 and 3:

$$\begin{aligned} &\textstyle\sum_{i=1}^n k_{y_i} r_i C_{\alpha_i} = 0, \quad \sum_{i=1}^n k_{y_i} r_i S_{\alpha_i} = 0 \\ &\textstyle\sum_{i=1}^n k_{z_i} r_i C_{\alpha_i} = 0, \quad \sum_{i=1}^n k_{z_i} r_i S_{\alpha_i} = 0. \end{aligned} \tag{10}$$

From (10), $\boldsymbol{K}_r$ results in

$$\boldsymbol{K}_r = \begin{bmatrix} \boldsymbol{K}_r^{pp} & \boldsymbol{0}_{3\times 3} \\ \boldsymbol{0}_{3\times 3} & \boldsymbol{K}_r^{\phi\phi} \end{bmatrix}. \tag{11}$$

From (7), (9), (11) and $\boldsymbol{K}_r^{pp} \succ 0$, the grasp is stable when the following holds:

$$\boldsymbol{K}_r^{\phi\phi} := \begin{bmatrix} A - MC_{\beta_g} & -D & MS_{\beta_g} \\ -D & B - MC_{\beta_g} & 0 \\ MS_{\beta_g} & 0 & C \end{bmatrix} \succ 0, \tag{12}$$

where

$$\begin{aligned} A &:= \textstyle\sum_{i=1}^n (r_i S_{\alpha_i} k_{z_i} - S_{\alpha_i} k_{x_i} \delta_{0x_i} - C_{\alpha_i} k_{y_i} \delta_{0y_i}) r_i S_{\alpha_i} \\ B &:= \textstyle\sum_{i=1}^n (r_i C_{\alpha_i} k_{z_i} - C_{\alpha_i} k_{x_i} \delta_{0x_i} + S_{\alpha_i} k_{y_i} \delta_{0y_i}) r_i C_{\alpha_i} \\ C &:= \textstyle\sum_{i=1}^n (k_{y_i} r_i - k_{x_i} \delta_{0x_i}) r_i \\ D &:= \textstyle\sum_{i=1}^n (r_i C_{\alpha_i} k_{z_i} - C_{\alpha_i} k_{x_i} \delta_{0x_i} + S_{\alpha_i} k_{y_i} \delta_{0y_i}) r_i S_{\alpha_i} \\ M &:= r_g m g. \end{aligned} \tag{13}$$

The terms A–C represent the stiffness effects about the x–z axes and D represents the interference effect between the x- and y-axes. M consists of the distance of the COG from the reference and the gravity. Therefore, M is called as the *gravity effect* in this paper. For the formulation of the stability problem, we define the following sets with respect to the position of the COG $x := C_{\beta_g}$:

$$\mathcal{R}_0 := \{\ x \mid -1 \le x \le 1\ \}, \mathcal{R}_j := \{\ x \mid f_j(x) > 0\ \}, \tag{14}$$

$$\mathcal{R}_{01} := \mathcal{R}_0 \cap \mathcal{R}_1,\ \mathcal{R}_{012} := \mathcal{R}_{01} \cap \mathcal{R}_2,\ \mathcal{R}_{0123} := \mathcal{R}_{012} \cap \mathcal{R}_3 \tag{15}$$

where $j = 1, 2, 3$ and

$$f_1(x) := -x + a \tag{16}$$

$$f_2(x) := (x-a)(x-b) - d^2 \tag{17}$$

$$f_3(x) := cf_2(x) - h(x),\ h(x) := (x^2-1)(x-b) \tag{18}$$

$$a := \frac{A}{M},\ b := \frac{B}{M},\ c := \frac{C}{M},\ d := \frac{D}{M}. \tag{19}$$

We call a–d as the *normalized stiffness effects* because they are defined the stiffness effect divided by the gravity effect M. Note that $f_j(x)$ is the determinant of the jth principal minor of $\boldsymbol{K}_r^{\phi\phi}$. From the Sylvester's criterion for the condition that (12) is positive definite, we formulate the stability problem with respect to the position of the COG:

Problem. Suppose $c > 0$. Find a necessary and sufficient condition on $\mathcal{R}_{0123} \neq \emptyset$ and then characterize the set of $\mathcal{R}_{0123}$ when the condition holds.

Remark 1. The physical meaning of the stability problem is illustrated in Fig. 2. Note that the angle α_g can be set to 0 for any x and y coordinates of the COG. Therefore, the position of the COG expressed by β_g with any x and y coordinates is characterized in the aqua surface area of the sphere with the radius M. For an example of $\pi/2 \le \beta_g^* \le \beta_g \le \pi$, the position area stands for the orange lower one. In the case of $0 \le \beta_g \le \pi$ ($-1 \le x \le 1$), the area of the position of the COG becomes all the one of the surface of the sphere. This means that the grasp is stable with any position of the COG.

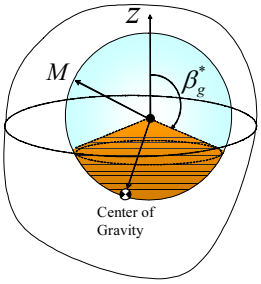

Fig. 2. Physical meaning of the stability problem.

This problem is solved in the next section.

3. MAIN RESULTS

Lemma 1. $\mathcal{R}_{01} \neq \emptyset$ is equivalent to $-1 < a$. Then,

$$\mathcal{R}_{01} = \begin{cases} \{\ x \mid\ -1 \le x < a\ \} & (a \le 1) \\ \{\ x \mid\ -1 \le x \le 1\ \} & (a > 1) \end{cases}. \tag{20}$$

Proof . From (14) and (16), $f_1(x) > 0$ leads to

$$\mathcal{R}_1 = \{x \mid x < a\}.$$

Since $\mathcal{R}_0 = \{x \mid\ -1 \le x \le 1\}$ of (14), $\mathcal{R}_{01} = \mathcal{R}_0 \cap \mathcal{R}_1$ of (15) is not an empty set iff $-1 < a$. If $a \le 1$, $\mathcal{R}_1 = \{x \mid x < a \le 1\}$. Then, $\mathcal{R}_{01} = \{x \mid\ -1 \le x < a\}$. If $a > 1$, the following holds:

$$\mathcal{R}'_{01} \subset \mathcal{R}_{01},\ \mathcal{R}'_{01} := \{x \mid\ -1 \le x \le a', -1 < a' < a\}.$$

$a' = 1$ leads to $\mathcal{R}_{01} = \mathcal{R}_0$. ∎

Lemma 2. $f_2(x) = 0$ has two real roots $e_2 < e'_2$ defined as

$$e_2 := \frac{a+b-\sqrt{(a-b)^2+4d^2}}{2}$$
$$e'_2 := \frac{a+b+\sqrt{(a-b)^2+4d^2}}{2}. \tag{21}$$

It follows that

$$e_2 < a < e'_2,\ e_2 < b < e'_2. \tag{22}$$

Proof . $f_2(x) = 0$ is rewritten as

$$x^2 - (a+b)x + ab - d = 0.$$

It is obvious that e_2 and e'_2 are the roots of the equation. The inequalities of a of (22) are proved by

$$a - e_2 = \frac{(a-b)+\sqrt{(a-b)^2+4d^2}}{2} > 0$$
$$a - e'_2 = \frac{(a-b)-\sqrt{(a-b)^2+4d^2}}{2} < 0.$$

The inequalities of b are easily proved by replacing a to b in the same proof. ∎

Lemma 3. $\mathcal{R}_{012} \neq \emptyset$ is equivalent to $-1 < e_2$. Then,

$$\mathcal{R}_{012} = \begin{cases} \{\ x \mid\ -1 \le x < e_2\ \} & (e_2 \le 1) \\ \{\ x \mid\ -1 \le x \le 1\ \} & (e_2 > 1) \end{cases}. \tag{23}$$

Proof . From (14) and (17), $f_2(x) > 0$ leads to

$$\mathcal{R}_2 = \{x \mid x < e_2,\ e'_2 < x\}. \tag{24}$$

Since $\mathcal{R}_1 = \{x \mid x < a\}$ and $e_2 < a < e'_2$ of (22),

$$\mathcal{R}_{12} := \mathcal{R}_1 \cap \mathcal{R}_2 = \{x \mid x < e_2\}.$$

From $\mathcal{R}_0 = \{x \mid\ -1 \le x \le 1\}$ of (14), $\mathcal{R}_{012} = \mathcal{R}_0 \cap \mathcal{R}_{12}$ of (15) is not an empty set iff $-1 < e_2$. The two cases of (23) are proved by the similar way as in Lemma 1. ∎

Lemma 4. Suppose Lemma 3 and $x \neq \pm 1, b$. Then, $h(x) > 0$.

Proof . From Lemma 3 and $x \neq \pm 1, b$,

$$\mathcal{R}_{012} = \begin{cases} -1 < x < e_2 & (e_2 \le 1) \\ -1 < x < 1 & (e_2 > 1) \end{cases}.$$

Since $-1 < e_2 < b$ from Lemma 2, the possibilities of the magnitude relation of $(-1, +1, b)$ are

$$-1 < 1 \le b \ \text{ or } \ -1 < b < 1.$$

Since $x = \pm 1, b$ are the roots of $h(x) = 0$,

$$\mathcal{R}_h := \{x \mid h(x) > 0\} \tag{25}$$

is characterized by

$$\mathcal{R}_h = \begin{cases} \{x \mid\ -1 < x < 1,\ b < x\} & (b \ge 1) \\ \{x \mid\ -1 < x < b,\ 1 < x\} & (b < 1) \end{cases}.$$

If $b \ge 1$, $\mathcal{R}_{012} \subset \mathcal{R}_h$ with any $e_2 > -1$. If $b < 1$, $\mathcal{R}_{012} \subset \mathcal{R}_h$ from $-1 < e_2 < b < 1$. ∎

Theorem 1. $\mathcal{R}_{0123} \neq \emptyset$ is equivalent to $-1 < e_2$. Then, $\mathcal{R}_{0123}$ is characterized by

$$\mathcal{R}_{0123} = \begin{cases} \{x \mid\ -1 \le x < p_1(c)\} & (e_2 \le 1) \\ \{x \mid\ -1 \le x < p_{21}(c) \text{ or } p_{22}(c) < x \le 1\} & (e_2 > 1) \end{cases}, \tag{26}$$

where $p_1(c)$, $p_{21}(c)$ and $p_{22}(c)$ are the roots of $f_3(x) = 0$ and

$$-1 < p_1(c) < e_2 \tag{27}$$
$$-1 < p_{21}(c) \le p_{22}(c) < 1. \tag{28}$$

$p_1(c)$ and $p_{21}(c)$ are monotone increasing and $p_{22}(c)$ is monotone decreasing. The followings hold:

$$\lim_{c \to +0} p_1(c) = -1,\ \lim_{c \to +\infty} p_1(c) = e_2 \tag{29}$$
$$\lim_{c \to +0} p_{21}(c) = -1,\ \lim_{c \to +\infty} p_{22}(c) = 1 \tag{30}$$

and there exist finite $c^* > 0$ and p_2^* such that

$$\lim_{c \to c^*} p_{21}(c) = \lim_{c \to c^*} p_{22}(c) = p_2^*. \tag{31}$$

Proof . From (14) and (18), $f_3(x) > 0$ leads to

$$\mathcal{R}_3 = \{x \mid c f_2(x) - h(x) > 0\}. \tag{32}$$

Let firstly consider the special cases $x = \pm 1, b$. Since $x = \pm 1, b$ are the roots of $h(x)$ and $c > 0$,

$$\mathcal{R}_{0123} = \mathcal{R}_{012}.$$

Therefore, from Lemma 3, $\mathcal{R}_{0123}$ is not an empty set when $-1 < e_2$.

Next consider the case of $x \neq \pm 1, b$. Since $h(x) > 0$ from Lemma 4, $\mathcal{R}_3$ of (32) results in

$$\mathcal{R}_3 = \{x \mid P(x) > 0\},\ P(x) := c\frac{f_2(x)}{h(x)} - 1. \tag{33}$$

Some properties of the root locus are used for the proof. The necessary ones are shown in Appendix A. Let the poles and zeros be $x_p = \pm 1, b$ and $x_z = e_2, e'_2$. Note that all the poles and zeros are on the real axis. Since $-1 < e_2 < b < e'_2$ from Lemmas 2 and 3, the possibilities of the magnitude relation of them are

(i) $-1 < e_2 < b < e'_2 < 1$ (ii) $-1 < e_2 < b < 1 < e'_2$
(iii) $-1 < e_2 < 1 < b < e'_2$ (iv) $-1 < 1 < e_2 < b < e'_2$.

By using Properties 1 and 2, the branches of the root locus of $P(x)$ in the cases of (i)–(iv) are depicted as in Figs. 3–6.

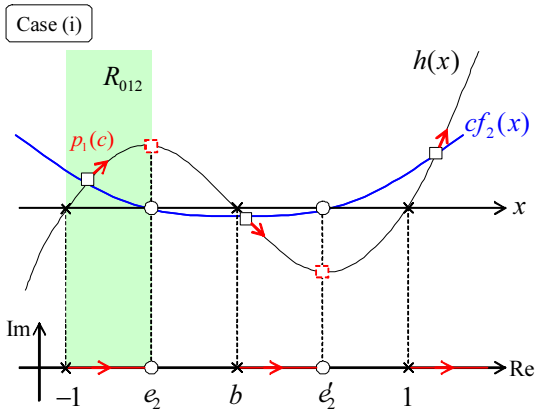

Fig. 3. The branches of the root locus in the case (i).

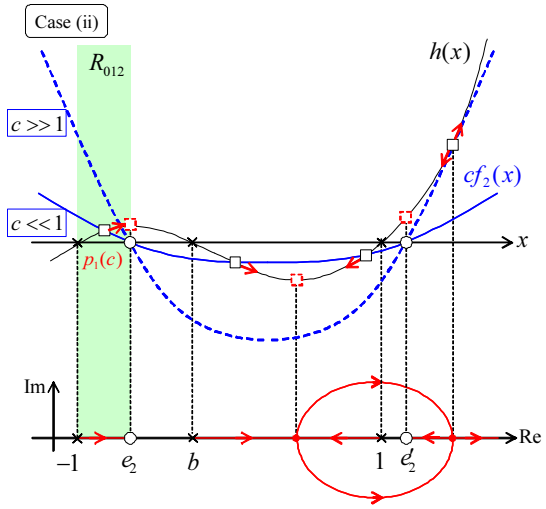

Fig. 4. The branches of the root locus in the case (ii).

Case (i) $[e_2 < 1]$**:** The upper and lower figures show the branches of the root locus in the complex plane and the behaviors of the roots expressed by the intersections of $cf_2(x)$ and $h(x)$. The poles and zeros are represented by the crosses and circles. In the lower figure, the red arrows represent the root locus branches. The two branches begin at the poles $x_p = -1, b$ and end at the zeros $x_z = e_2, e_2'$ respectively. The other one begins at the pole $x_p = 1$ and approaches a zero at infinity. These behaviors of the roots are depicted by the squares in the upper figure. The black and blue lines represent $h(x)$ and $cf_2(x)$. The red arrows are the directions of the root movements when c increases. The dashed red squares are the convergent roots when $c = +\infty$. The green area represents $\mathcal{R}_{012}$. Therefore, $\mathcal{R}_{0123}$ is given by $\{x \mid -1 < x < p_1(c)\}$ as in (26). The branch from $x_p = -1$ to $x_z = e_2$ yields (27) and (29). From (27), $\mathcal{R}_{0123}$ is not an empty set iff $-1 < e_2$.

Case (ii) $[e_2 < 1]$**:** The configurations and marks in Fig. 4 are the same as Fig. 3. Note that the solid and dashed blue lines represent $cf_2(x)$ in the cases of $c \ll 1$ and $c \gg 1$ respectively. In this case, there is a breakaway point between b and 1. One of the two branches from the point has to end at the zero $x_z = e_2'$ and the other has to approach a zero at infinity. Since these have to be symmetric, there is a break-in point in the section to the right of $x_z = e_2'$. Since the relation between $p_1(c)$ and $\mathcal{R}_{012}$ and the properties of $p_1(c)$ are the same in Case (i), the proof is the same.

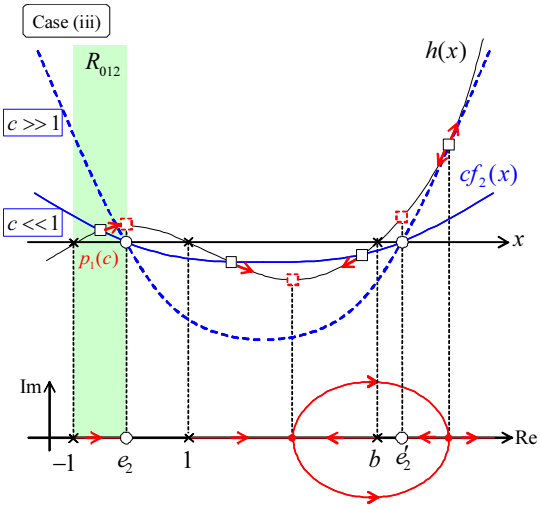

Fig. 5. The branches of the root locus in the case (iii).

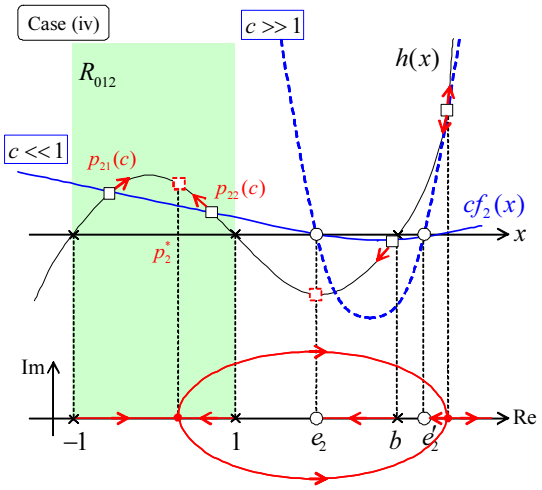

Fig. 6. The branches of the root locus in the case (iv).

Case (iii) $[e_2 \leq 1]$**:** The locations of the zeros $x_z = 1, b$ are changed each other compared with Case (ii). All the other things are the same.

Case (iv) $[1 < e_2]$**:** In this case, there are the two roots $p_{21}(c)$ and $p_{22}(c)$ in $\mathcal{R}_{012}$. Therefore, $\mathcal{R}_{0123}$ is given by $\{x \mid -1 < x < p_{21}(c)$ or $p_{22}(c) < x < 1\}$ as in (26). Since there is a breakaway point p_2^* given by $c = c^* < \infty$ of the roots $p_{21}(c)$ and $p_{22}(c)$ between -1 and 1, the branches from $x_p = \pm 1$ yield (28), (30) and (31). ∎

Remark 2. The areas of the position of the COG in the cases of $e_2 \leq 1$ and $1 < e_2$ are illustrated as the orange ones in Fig. 7. The angles of the areas are defined as

$$\beta_1(c) := \cos^{-1} p_1(c), \ \beta_{2i}(c) := \cos^{-1} p_{2i}(c), i = 1, 2. \quad (34)$$

From the properties of (27)–(31), the areas are enlarged by increasing c. Especially, in the case of $1 < e_2$, the area of the position of the COG is the sphere with the radius M by a finite c^* because the two areas of β_{21} and β_{22} become the one area at $\beta_{21}(c^*) = \beta_{22}(c^*)$. Then, the grasp is always stable with any position of the COG.

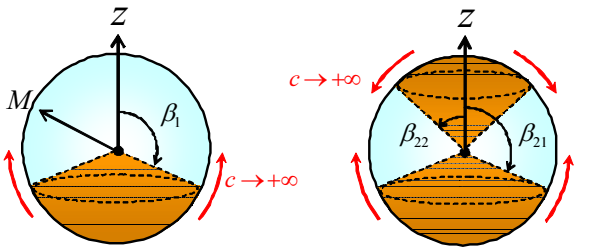

(a) The case of $e_2 \le 1$ (b) The case of $1 < e_2$

Fig. 7. The areas of the position of the COG.

Remark 3. Let us characterize the conditions shown in Theorem 1 with respect to the normalized stiffness effects a, b and d. From (21), the equivalent condition of $\mathcal{R}_{0123} \neq \emptyset$, i.e., $-1 < e_2$, results in

$$(a+1)(b+1) > d^2. \tag{35}$$

Furthermore, the conditions characterizing $\mathcal{R}_{0123}$, i.e., $e_2 \le 1$ and $1 < e_2$, result in

$$(a-1)(b-1) \le d^2,\ (a-1)(b-1) > d^2. \tag{36}$$

The conditions of (35) and (36) are depicted in Fig. 8. The bold solid curves represent $e_2 = -1$ and $e_2 = 1$. The curve of $e_2 = -1$ asymptotically converges to the lines $a, b = -1$ and has the intersection points $a = d^2 - 1$ and $b = d^2 - 1$. That is, the stable area of (a, b) includes negative values of a and b. Therefore, even if one of (a, b) is negative, the grasp can be stable when the other is positive large. The curve of $e_2 = 1$ asymptotically converges to the lines $a, b = 1$. Therefore, the magnitudes of a and b have to be at least greater than 1 in the stable area of (a, b) of $1 < e_2$. This means that the stiffness effects A and B are necessary to be greater than the gravity effect M in order to realize the stable grasp with any COG position because $a = A/M$ and $b = B/M$.

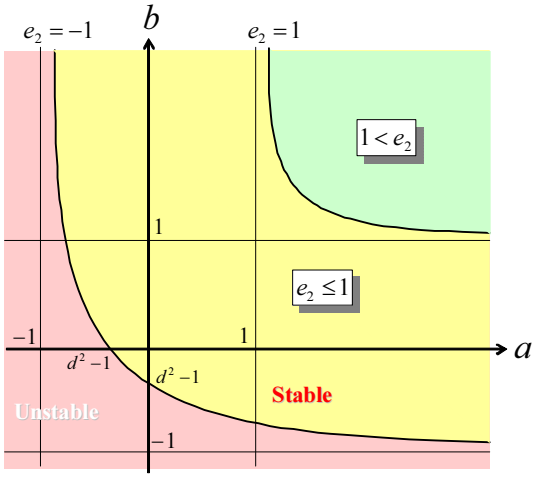

Fig. 8. The characterized areas of a and b.

4. NUMERICAL EXAMPLES

Some numerical examples are carried out in this section. The setting of the examples is show in Fig. 9. The figure (a) is the overview of the grasp situation, where the hand has three fingers and the grasped object is a cylinder. The figure (b) shows the configurations of the reference frame Σ_B and spring frame Σ_{S_i}. The mass of the object is $m = 132$ [g] and the distance of the COG is $r_g = 33.5$ [mm]. The distance of Σ_{S_i} from Σ_B is $r_i = 37.5$ [mm]. In the latter, we check the area of the position of the COG with some parameter of the contact point α_i, the initial displacement of the spring $\boldsymbol{\delta}_{0_i}$ and the stiffness coefficients $(k_{x_i}, k_{y_i}, k_{z_i})$.

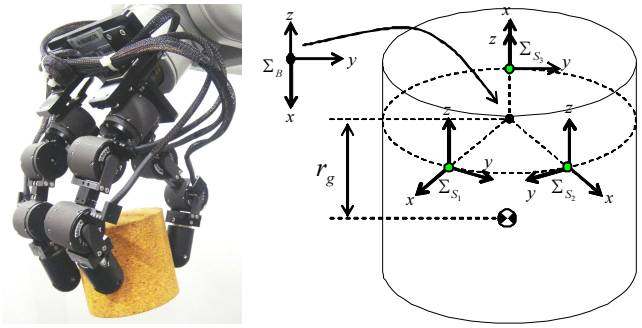

(a) Overview of the grasp situation. (b) The configurations of the frames.

Fig. 9. The setting of the numerical examples.

First, the contact parameters are set to $\alpha_1 = -\alpha_2 = 60$ and $\alpha_3 = 180$ [deg]. This configuration is symmetric because the triangle whose the apexes are the contact points is equilateral The initial displacements are set to $\boldsymbol{\delta}_{0_i} = [20, 0, -2]^{\mathrm{T}}$ $(i = 1, 2, 3)$. The stiffness coefficients are changed as (1-a) $k_{x_i} = 433$, (1-b) $k_{x_i} = 355$, (1-c) $k_{x_i} = 217$ and the others are set to $k_{y_i} = k_{z_i} = 200$ [N/m] $(i = 1, 2, 3)$. Figure 10 shows the results of the stability analyses. The 1st, 2nd and 3rd rows are the cases (1-a)–(1-c) respectively. The left and right figures represent the stiffness effects (a, b) and the positions of the COG. In the left figures, the red circles are (a, b) and the red and blue lines represent the conditions of $e_2 = -1$ and $e_2 = 1$. Note that $e_2 = -1$ means the boundary of the stable or unstable. In the right figures, the blue circles represent the spheres with the radii M and the areas surrounded by the orange lines represent the position of the COG of the stable grasp. The grasp of (1-a) is unstable while the others are stable. It is confirmed that the grasp can be unstable with a big k_{x_i} from the result of (1-a). Furthermore, from the results of (1-a) and (1-b), the stable area of the position of the COG is enlarged by decreasing k_{x_i}. Note that k_{x_i} and δ_{0x_i} are redundant parameters of the grasp which corresponds to the *internal force*. From the results, the smaller internal force is effective for the stable grasp. However, the internal force is necessary to be enough large in order to satisfy the friction condition. Therefore, it is important to take into account this trade-off when the fingers grasp the object.

Next, we change the contact parameters from the one of (1-b) as (2-a) $\alpha_1 = -\alpha_2 = 60$ and $\alpha_3 = 120$ and (2-b) $\alpha_1 = -\alpha_2 = 45$ and $\alpha_3 = 180$ [deg]. The results are shown in Fig. 11. In the case (2-a), the symmetry is broken by changing the α_3. It is confirmed that the stable area becomes narrower from $\beta_g^* = 109$ to 118 [deg]. In the case (2-b), the symmetry is conserved but the distance between the contact points 1, 2 becomes narrower. It is confirmed that the stable area becomes quite small one

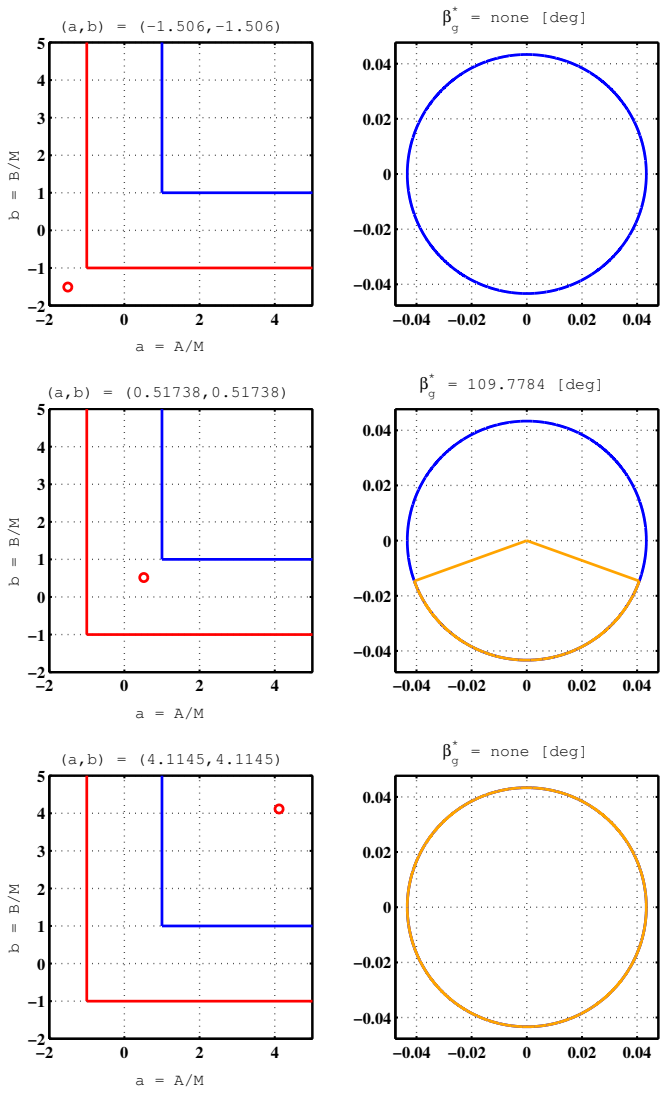

Fig. 10. The numerical examples with the changed k_{x_i}.

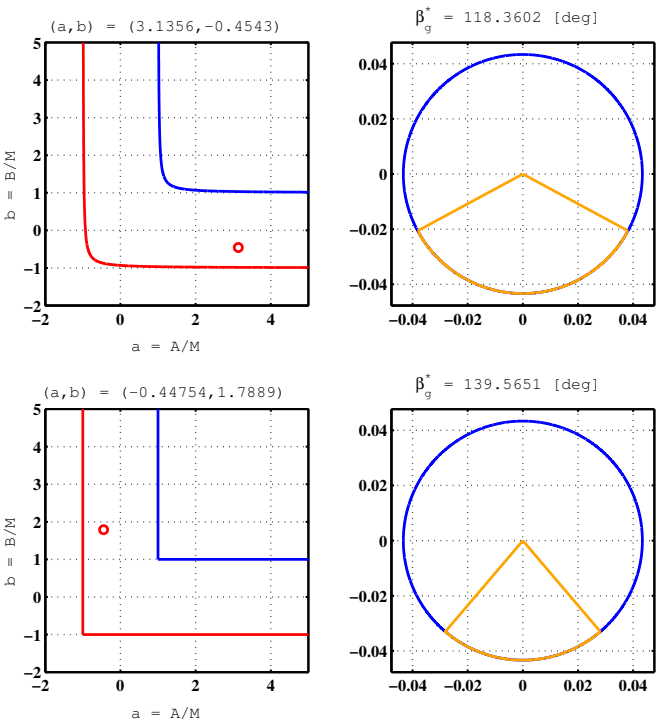

Fig. 11. The numerical examples with the changed α_i.

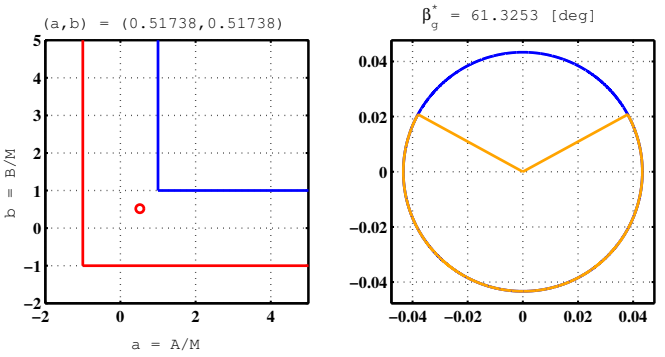

Fig. 12. The numerical example with the changed k_{y_i}.

with $\beta_g^* = 140$ [deg]. These results indicate that it is more important to enough distances between the contact points than the symmetry of those.

Finally , the example that the k_{y_i} is changed to be twice is shown in Fig. 12. The other parameters are the same as the example of (1-b). It is confirmed that the stable area is enlarged by the bigger k_{y_i}. This is because the stiffness effect c is changed from 1 to 20.5 from Remark 2. However, since enlarging c increases the tangent forces to the object surface at the contact points, too big c may break the friction condition. Therefore, this is also the trade-off problem and has to be determined carefully.

5. CONCLUSIONS

In this paper, we dealt with the stability analysis of an object grasped by fingers with linear stiffness in the case where the gravity effect is considered. The analysis problem was formulated as finding a condition of the stiffness parameters and contact points for the position of the COG to exist such that the grasp is stable. A necessary and sufficient condition was derived under assumptions with respect to the stiffness and contact points. Furthermore, on the derived condition, the position of the COG was characterized with respect to the stiffness and contact points. Numerical examples were shown to prove the effectiveness of the analysis.

In the numerical examples, two trade-off problems are indicated. The optimization problem of the parameters with the trade-offs is feature work. As a similar problem, the reagion analysis of the object orientation is important because the grasped object may be put on with any orientation in the situation of pick-and-place. Note that the parameters consist of the stiffness coefficients, initial spring displacement and contact points. In fact, there are some errors of the parameters when a hand robot grasps an object. Therefore, analysis of the parameter robustness is another feature work.

REFERENCES

Abell, T. and Erdmann, M. (1995). Stably supported rotations of a planar polygon with two frictionless con-

tacts. In *Proc. IEEE/RSJ Int. Conf. Intel. Robot. Sys.*, volume 3, 411 –418 vol.3.

Arimoto, S., Doulgeri, Z., Nguyen, P.T.A., and Fasoulas, J. (2002). Stable pinching by a pair of robot fingers with soft tips under the effect of gravity. *Robotica*, 20, 241–249.

Arimoto, S. (2008). *Control Theory of Mult-fingered Hands*. Springer.

Baraff, D., Mattikalli, R., and Khosla, P. (1997). Minimal fixturing of frictionless assemblies: Complexity and algorithms. *Algorithmica*, 19, 4–39.

Cheah, C.C., H.-Y, H., Kawamura, S., and Arimoto, S. (1998). Grasping and position control for multi-fingered robot hands with uncertain jacobian matrices. In *Proc. IEEE Int. Conf. Robot. Automat.*, 2403–2408.

Cole, A.B.A., Hauser, J.E., and Sastry, S.S. (1989). Kinematics and control of multifingered hands with rolling contact. *IEEE Trans. Automat. Contr.*, 34(4), 398–404.

Cutkosky, M. and Kao, I. (1989). Computing and controlling the compliance of a robot hand. *IEEE Trans. Robot. Automat.*, 5(2), 151–165.

Hanafusa, H. and Asada, H. (1977). Stable prehension by a robot hand with elastic fingers. In *Pric. 7th Int. Symp. on Industrial Robots*, 361–368.

Howard, W.S. and Kumar, V. (1996). On the stability of grasped objects. *IEEE Trans. Robot. Automat.*, 12(6), 904–917.

Kaneko, M., Imamura, N., Yokoi, K., and Tanie, K. (1990). A realization of stable grasp based on virtual stiffness model by robot fingers. In *Proc. IEEE Int. Workshop on Adv. Mtn Cont.*, 156–163.

Kerr, J. and Roth, B. (1986). Analysis of multifingered robot hands. *Int. J. Robot. Res.*, 4(4), 3–17.

Li, Z. and Sastry, S.S. (1988). Task-oriented optimal grasping by multifingered robot hands. *IEEE J. Robot. Automat.*, 4(1), 32–44.

Magialardi, L., Mantriota, G., and Trentadue, A. (1996). A three-dimensional criterion for the determination of optimal grip points. *Robot. Computer-Integrated Man.*, 12(2), 157–167.

Markenscoff, X. and Papadimitriou, C.H. (1989). Optimum grip of a polygon. *Int. J. Robot. Res.*, 8(2), 17–29.

Mattikalli, R., Baraff, D., Khosla, P., and Repetto, B. (1995). Gravitational stability of frictionless assemblies. *IEEE Trans. Robot. Automat.*, 11(3), 374 –388.

Montana, D.J. (1992). Contact stability for two-fingered grasps. *IEEE Trans. Robot. Automat.*, 8(4), 78–85.

Murray, R.M., Li, Z., and Sastry, S.S. (1994). *A Mathematical Introduction to ROBOTIC MANIPULATION*. CRC Press.

Nagai, K. and Yoshikawa, T. (1993). Dynamic manipulation/grasping control of multifingered robot hands. In *Proc. IEEE Int. Conf. Robot. Automat.*, 1027–1032.

Nakamura, Y., Nagai, K., and Yoshikawa, T. (1989). Dynamics and stability in coordination of multiple robotic mechanisms. *Int. J. Robot. Res.*, 8(2), 44–61.

Nakashima, A., Shibata, T., and Hayakawa, Y. (2009). Control of grasp and manipulation by soft-finger with 3-dimensional deformation. *SICE JCMSI*, 2(2), 78–87.

Nakashima, A., Yoshimatsu, Y., and Hayakawa, Y. (2010). Analysis and synthesis of stable grasp by multi-fingered robot hand with compliance control. In *Proc. IEEE Int. Multi Conf. Sys. Cont.*, 1582–1589.

Nguyen, V. (1988). Constructing force-closure grasps. *Int. J. Robot. Res.*, 7(3), 3–16.

Ogata, K. (1990). *Modern Control Engineering*. Prentice-Hall, 2 edition.

Sarkar, N., Yun, X., and Kumar, V. (1997). Dynamic control of 3-d rolling contacts in two-arm manipulation. *IEEE Trans. Robot. Automat.*, 13(3), 364–376.

Svinin, M., Ueda, K., and Kaneko, M. (1999). Analytical conditions for the rotational stability of an object in multi-finger grasping. In *IEEE Int. Conf. Robot. Automat.*, volume 1, 257 –262 vol.1.

Watanabe, T. and Yoshikawa, T. (2003). Optimization of grasping an object by using required acceleration and equilibrium-force sets. In *Proc. IEEE/ASME Int. Conf. Adv. Intel. Mech.*, 338–343.

Yamada, T., Kuraishi, T., Mizuno, Y., Mimura, N., and Funahashi, Y. (2001). Stability analysis of 3d grasps by a multifingered hand. In *Proc. IEEE Int. Conf. on Robot. Automat.*, 2566–2473.

Yoshikawa, T. and Nagai, K. (1991). Manipulating and grasping forces in manipulation by multifingered robot hands. *IEEE Trans. Robot. Automat.*, 7(1), 67–77.

Zheng, X.Z., Nakashima, R., and Yoshikawa, T. (2000). On dynamic control of finger sliding and object motion in manipulation with multifingered hands. *IEEE Trans. Robot. Automat.*, 16(5), 469–481.

Zumel, N. and Erdmann, M. (1996). Nonprehensile two palm manipulation with non-equilibrium transitions between stable states. In *Proc. Int. Conf. Robot. Automat.*, volume 4, 3317 –3323 vol.4.

Appendix A. PROPERTIES OF ROOT LOCUS

The properties of the root locus are shown in usual control textbooks, e.g., see the book by Ogata (1990). The properties used in this paper are picked up here.

Let us consider the root locus of the following characteristic equation:

$$KG(s) - 1 = 0,\ G(s) := \frac{N(s)}{D(s)},\ K \geq 0. \tag{A.1}$$

Define p_i $(i = 1, \cdots, M_p)$ and z_j $(j = 1, \cdots, M_z)$ are the poles and zeros of $G(s)$, i.e., $D(p_i) = N(z_j) = 0$. Suppose that $M_p > N_p$ and the poles and zeros are different from each other. When K is increasing from 0 to $+\infty$, some properties of the root locus in the complex plane are given by the followings:

Property 1. There exist M_p branches of the root locus of (A.1) which are symmetric with respect to the real axis. The branches begin at the poles p_i at $K = 0$. M_z branches end at the zeros z_j at $K = +\infty$ and the other branches approach the $M_p - M_z$ zeros at infinity.

Property 2. Suppose that there exist some poles and zeros on the real axis. The root locus on the real axis always lies in a section of the real axis to the left of an even number of poles and zeros.

Note that the sign of 1 of (A.1) is positive in usual formulations and in the case of $+1$ "even" has to be replaced to "odd." in Property 2.